Astron. Astrophys. 350, 310–317 (1999)

ASTRONOMY AND ASTROPHYSICS

Quadrupole moment of the Sun. Gravitational and rotational potentials

Stéphany Godier and Jean-Pierre Rozelot

Observatoire de la Côte d'Azur, Département CERGA UMR 6527 du CNRS, av. Copernic, F-06130 Grasse, France (godier,rozelot@obs-azur.fr)

Received 15 March 1999 / Accepted 9 July 1999

Abstract. The solar quadrupole moment J_2 was computed taking into account an up-to-date solar model of mass and density, combined with a recent rotational model established from the helioseismic data, and including the effects of differential rotation with depth. To determine precisely the theoretical value of J_2 of the Sun, we integrated the extended differential equation governing the fluids in hydrostatic equilibrium, and the Poisson equation for the gravitational potential. From this analysis, we deduced the profiles of J_2, as a function of the radius and of the latitude, from the core to the surface. This study has given information on the distortion of the total potential which accounts for the gravitational and rotational potentials.

As a result of our analysis, we found $J_2 = 1.60.10^{-7}$ which respects the upper bound $J_{2\,\max} = 3.0.10^{-6}$ derived from the best knowledge of the Moon's physical librations. Finally, we linked the profiles of J_2 within the Sun to the solar interior structure mainly governed by the shear in the tachocline and just below the surface.

Key words: Sun: fundamental parameters – Sun: interior – Sun: rotation – Sun: transition region

1. Introduction

The aim of this study is to investigate the behavior of the quadrupole moment of the Sun, via its gravitational and rotational potentials. The shape of the profile of J_2, as a function of the radius from the center to the surface, and the determination of its theoretical value at the surface establish J_2 as a non negligible solar quantity. First, this quantity provides information on the distortion of the total solar potential as J_2 is its first perturbation coefficient. Next, it should be used as a new constraint in the computation of solar models, as the asphericity is a probe to test the solar interior. Finally, it should be linked to the motion of the planets, as the orbital planes of the planets do not coincide with the Sun's rotational equator. This is specially the case for the motion of Mercury's orbit and J_2 should be accounted for in the calculations of the ephemeris of the planets.

Several studies and observations have already been made to determine J_2, mainly in the 70s and in the 80s, but without conclusive results. As early as 1966, Dicke undertook observations with the Princeton Solar Distortion Telescope and was able to measure the ellipticity of the Sun for the first time. He found a value for J_2 as large as $(2.47 \pm 0.23).10^{-5}$, a revised value deduced from the original data (Dicke & Goldenberg, 1967) taking into account all corrections for the seeing effects (Dicke & Goldenberg, 1974). Such a result has raised many questions concerning the astrophysical consequences along with the observations and their significance. Since then, several other determinations were made. In 1968, Goldreich and Schubert show that the maximum solar oblateness consistent with the stability of the Sun is $3.5.10^{-4}$ which yields, according to Hill et al. (1982) $J_2 = (5.5 \pm 1.3).10^{-6}$. At that time, they demonstrated that the value of J_2 was insensitive to the rotation laws. However, non monotonic rotation curves, forced to fit the helioseismic data, yield smaller values for J_2: such a procedure yields $(1.0 \pm 4.3).10^{-6}$ (Hill & Stebbins, 1975) as the best value for J_2. In 1981, Ulrich and Hawkins made a theoretical computation of J_2 and J_4, taking into account the differential rotation and using the theory of the solar gravitational figure. They found $1.0.10^{-7} \leq J_2 \leq 1.5.10^{-7}$ and $2.10^{-9} \leq J_4 \leq 5.10^{-9}$. In 1983, Kislik considering the Sun rotating as a rigid ellipsoid of revolution gave a theoretical range of J_2 equal to: $0 \leq J_2 \leq 1.08.10^{-5}$ and studied its effects, via the oblateness, on the planetary orbits. This same year, Campbell et al. (1983) determined from rotational splittings of global oscillations of the Sun, the minimum quadrupole moment coefficient: $J_2 = 1.6.10^{-6}$ and compared it with the general relativity and the nonsymmetric theory of gravitation. In Burša 1986, estimated an upper limit $|J_2| < 1.1.10^{-5}$ (Bursa, 1986). In 1992, Landgraf determined $|J_2| = (0.6 \pm 5.8).10^{-6}$ from astrometric observations of the minor planet Icarus (Landgraf, 1992). Based on the same type of observations (astrometric determination of the orbital elements of Icarus), Lieske and Null (1969) have estimated J_2 as $(1.8 \pm 2.0).10^{-5}$. Also in 1992, Maier et al. made observations with the Solar Disk Sextant (SDS), an instrument on board a balloon flight which measured the solar diameter at different orientations. From this experiment, Lydon & Sofia (1996) deduced a value of $1.8.10^{-7}$ for J_2 and $9.8.10^{-7}$ for J_4. More recently, Rösch et al. (1996) proposed from their observations with the scanning heliometer at the Pic-du-Midi observatory, a new estimation of J_2, i.e. $(2.57 \pm 2.36).10^{-6}$. To test these observational values, Rozelot & Bois (1998) proposed a new

theoretical value for the upper bound $J_2 < 3.0.10^{-6}$, given by the Moon's physical librations which are accurately determined (at the milliarcsecond level) with the help of Lunar Laser Ranging data. Finally, in Paternó et al. 1996, , using only one value of the ellipticity of the Sun (derived from the SDS experiment), presented a table of values for the quadrupole moment which varies between $2.15.10^{-7}$ and $3.83.10^{-7}$. They attempted to take into account the constraints on the rotation given by the lastest data in helioseismology, but the rather empiric law used in their paper did not reflect directly the observations made over all the heliographic latitudes.

This last remark justifies the decision of undertaking a new study to determine J_2, using one of the most recent solar models of mass and density combined with an up-to-date rotational model, which depends both on the distance to the rotation axis and on the latitude. This rotational model derives from the helioseismological observations of *p*-mode rotational frequency splitting, obtained by means of the SOHO spacecraft.

In the following sections, we present the theoretical method of calculation and the models used to obtain J_2. Next, we give the results and their interpretations; finally, we discuss the relation between the behavior of J_2 and some particular mechanisms inside the Sun.

2. Theoretical approach

In this work, we reconsider the theory of a solar gravitation figure to include the effects of differential rotation. Let us recall that the quadrupole moment is defined as a dimensionless coefficient in the perturbation expression of the gravitational potential. The study begins with the basic figure for steady rotation around a fixed axis (forming the zero-order approximation); then, small corrections are successively added to obtain the best shape of the Sun. The problem of finding this shape with a very high accuracy requires exact definition of the surface of the Sun. The generally accepted assumption is that this surface is of constant gravitational potential. So, the gravitational potential is developed in spherical harmonics linked to Legendre polynomials P_n. Since the figure shows the symmetry created by the rotation around the minor axis, only even polynomials P_{2n} appear in the gravitational potential expression U_G:

$$U_G = -\frac{GM_\odot}{R_E}\left[\frac{R_E}{r} - \sum_{n=1}^{\infty} J_{2n}\left(\frac{R_E}{r}\right)^{2n+1} P_{2n}(\cos\theta)\right] \quad (1)$$

where G is the gravitational constant, R_E the equatorial radius, $M_\odot$ the solar mass, r the solar radial vector (taken here as a variable), P_{2n} the Legendre polynomials, θ the colatitude and J_{2n} the coefficients associated to the dynamical form of the Sun. The zonal harmonic coefficient of degree 2 (J_2) is the quadrupole moment, whereas n=2 leads to an hexadecapole term (J_4, which is neglected in a first approach). Successive terms in the expansion of Expression 1 introduce finer details of the figure of the Sun. To this gravitational potential must be added the potential due to the rotation (w) of the Sun. Retaining only first order terms, and substituting $P_2(\cos\theta)$ by its value, the total potential becomes:

$$U_T = -\frac{GM_\odot}{R_E}\left[\frac{R_E}{r} - \frac{J_2}{2}\left(\frac{R_E}{r}\right)^3 (3\cos^2\theta - 1)\right] - \frac{1}{2}w^2 r^2 \cos^2\theta \quad (2)$$

By definition of the surface, U_T is the same whatever θ is. If r is known at least for two latitudes θ_1 and θ_2, this expression allows us to obtain J_2 by writing $U_{T_1} = U_{T_2}$. This was done for example by Brouillet (1997), but solar observations (of the radius) of very high precision are required to deduce J_2 with very high accuracy. Our approach will be slightly different by writing that for a given r, U_G is continuous from the interior to the exterior, that is to say at the surface. This is determined by a relevant differential equation, which can be easily derived under the assumption of hydrostatic equilibrium. This assumption is based on the rearrangement of the gravitational potential within the Sun. It can be internally heterogeneous, but the condition of hydrostatic equilibrium allows us to suppose that the internal density is uniform over the surface. The heterogeneous composition is represented as a series of thin shells, the composition of each shell being homogeneous. The gravitational potential within the Sun is solely related to the surfaces of constant density because it depends on the resultant gravitational interaction between all the constituent parts of the Sun (Roxburgh, 1964). In spherical polar coordinates $\frac{\partial P}{\partial r}$ and $\frac{\partial P}{\partial \theta}$ can be expressed as functions of ρ, Φ and Ω (see Eqs. 5. and 6. in Paternó et al. 1996).

Expanding the gravitational potential Φ in the form:

$$\Phi = \phi_0(r) + \phi_2(r,\theta)P_2(\cos\theta) \quad (3)$$

where ϕ_2 is a first order term, the differential equation (9) given in the above quoted paper becomes now:

$$\frac{d^2y}{dx^2} + \frac{2}{x}\frac{dy}{dx} - \frac{(6+UV)}{x^2}y = \frac{UV}{3}w^2 + \frac{2Uw}{3}\left(x\frac{dw}{dx} + \tan\theta\frac{dw}{d\theta}\right) \quad (4)$$

where the quantities $x = \frac{r}{R_\odot}$ and $y = \frac{\phi_2(r,\theta)}{\Omega_\odot^2 R_\odot^2}$ have been introduced dimensionless, as well as $U(x) = \frac{4\pi\rho R_\odot^3 x^3}{M_\odot M_x}$, $V(x) = \frac{d\ln\rho}{d\ln x}$ and $w(x,\theta) = \frac{\Omega(x,\theta)}{\Omega_\odot}$. It might be relevant to point out that the latitudinal variation of $\Omega = \Omega(x,\theta)$, the angular velocity, is taken into account in Eq. 4 for the first time due to the recent progress of the rotational models derived from the helioseismic data. Note, that our reference angular velocity is taken from the radiative region which rotates as a rigid body at the rate $\Omega_\odot = 435nHz$.

The boundary conditions are obviously the same as described in the paper of Paternó et al., whatever θ is, i.e. in a dimensionless form: $y = 0$ at $x = 0$ and $3y + x\frac{dy}{dx} = 0$ at $x = 1$.

As

$$\phi_2(r,\theta) = J_2\left(\frac{R_\odot}{r}\right)^2 \frac{GM_\odot}{r} \quad (5)$$

it follows that

$$J_2 = \frac{\phi_2(r,\theta)}{R_\odot^2 \Omega_\odot^2} \frac{\Omega_\odot^2 r^3}{GM_\odot} \quad (6)$$

or

$$J_2 = y(r,\theta) \frac{\Omega_\odot^2 r^3}{GM_\odot} \quad (7)$$

As we consider in this paper the Sun made up of successive thin shells of thickness dr, we compute J_2 for every shell assuming that the matter which is outside a shell of a given radius $r'_\odot$, is in space. The shell located at the radius $r'_\odot$ contains the whole internal mass $M'_\odot$ and each shell is considered as an equipotential surface with a homogeneous density. Thus, the quadrupole moment for a shell is given by:

$$J'_2 = y(r'_\odot,\theta) \frac{\Omega'^2_\odot r'^3_\odot}{GM'_\odot} \quad (8)$$

where $r'_\odot$, $M'_\odot$, $\Omega'_\odot$ are respectively the radius, the mass and the reference rotation rate of a shell and the above mentioned boundary conditions are applicable on each of these shells. To obtain the total quadrupole moment, J'_2 is integrated over the solar radius at a given latitude and then, over the latitude.

To solve the differential Eq. 4, we need a mass and density model for the Sun. We have chosen one of the five solar models computed by Richard et al. (1996) including the helioseismological constraints and element segregation (Model 3).

As the solar rotation depends both on the radial distance and on the colatitude, we need to define a law to express $\Omega(r,\theta)$. Among several laws available, we have chosen that proposed by Kosovichev (1996b), which is based on the observed *p*-mode rotational frequency splittings. The law is represented in terms of associated Legendre functions of order 1, $P_k^1(\theta)$:

$$\frac{\Omega(r,\theta)}{2\pi} = \sum_{k=0,1,2} \alpha_k A_{2k+1}(r) \frac{P^1_{2k+1}(\theta)}{\sin\theta} \quad (9)$$

where

$$\alpha_k = (-1)^{(k+1)} \frac{k!2k}{(2k+1)!!} \quad (10)$$

and A_k(r) is a radial function developed in a parametric form. From the analysis of the Big Bear Solar Observatory data, Kosovichev formulates a simple model of solar rotation based on the first three terms in the expansion of Eq. 9 ($x = \frac{r}{R_\odot}$):

$$\begin{aligned}\frac{\Omega(r,\theta)}{2\pi} &= A_1(x) + A_3(x)\left[1\text{–}5\cos^2\theta\right] \\ &\quad + A_5(x)\left[1\text{–}14\cos^2\theta + 21\cos^4\theta\right]\end{aligned} \quad (11)$$

From a numerical point of view, with the value of A_k given in nHz, Eq. 11 is expressed by:

$$A_1(x) = \left\{ \begin{array}{rl} 435 & x \le 0.71 \\ 435 + 51.85(x-0.71) & 0.71 \le x \le 0.983 \\ 435\text{–}882.53(x-1) & 0.983 \le x \le 1 \end{array} \right\} \quad (12)$$

$$A_3(x) = 22\phi(x) \quad (13)$$

$$A_5(x) = -3.5\phi(x) \quad (14)$$

where

$$\phi(x) = 0.5\left(1 + \mathrm{erf}\left[2\frac{(x-0.69)}{0.1}\right]\right) \quad (15)$$

This model is particularly useful, because it describes fairly well the differential rotation of the convective zone and the rigid rotation of the radiative zone. But, due to the lack of data concerning the *g*-modes, it is not yet possible to know if the rotation in the core is faster or slower than the rotation of the radiative zone. Thus, we adopt the same rotation rate for the core and for the radiation zone: ∼435 nHz. Consequently, we have no access to the quadrupole moment J_2 of the shells, inside the core region of the Sun, i.e. from the center up to $0.25R_\odot$, a value which is approximately the upper limit of the core surface. To check this assertion, we made some computations by choosing different rotation rates for the core (faster and slower than the rotation rate of the radiation zone) in order to evaluate J_2 and to estimate its variation with this change of the core rotation rate (see Sect. 3.3, Eq. 23 and after).

3. Determination of the quadrupole moment of the Sun

3.1. Outline of the calculations

The differential Eq. 4 can be solved in the form

$$y(x) = C_1 \exp(\tau_1 x) + C_2 \exp(\tau_2 x) + C_0 \quad (16)$$

where τ_1 and τ_2 are the roots of the characteristic equation. Bearing in mind the boundary conditions, C_1, C_2 and C_0 (a particular solution) can be expressed as:

$$C_1 = \frac{C_0\left[(\tau_1 x + 3)\exp(\tau_1 x) - 3\right]}{(\tau_1 x + 3)\exp(\tau_1 x) - (\tau_2 x + 3)\exp(\tau_2 x)} \quad (17)$$

$$C_2 = -\frac{C_0\left[(\tau_2 x + 3)\exp(\tau_2 x) - 3\right]}{(\tau_1 x + 3)\exp(\tau_1 x) - (\tau_2 x + 3)\exp(\tau_2 x)} \quad (18)$$

and

$$C_0 = -\frac{\frac{UV}{3}w^2 + \frac{2Uw}{3}\left(x\frac{dw}{dx} + \tan\theta\frac{dw}{d\theta}\right)}{(6+UV)/x^2} \quad (19)$$

Through Eq. 8, we deduce the behavior of J_2, shell by shell, the numerical integration step being determined by the model (the interval range of r being sampled by 220 values). For the numerical applications, the adopted values for the solar parameters are those given by Allen (1976): $R_\odot = 6.95997.10^8 m$ and $M_\odot = 1.9892.10^{30} kg$.

3.2. The rigid solar rotation case

The case $w = 1$, which is the case of a Sun rotating as a rigid body, is easy to treat and highlights at least two important features which have not been mentioned yet. They are illustrated

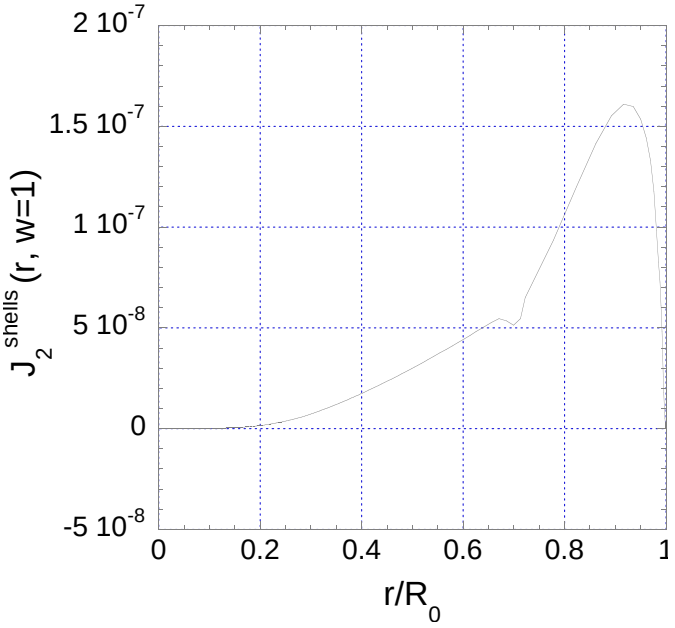

Fig. 1a. Profile of the quadrupole moment splitted into successive shells and numerically computed for the case $w = 1$ (rigid rotation). Around $0.7R_\odot$, the passage of the transition zone is clearly visible.

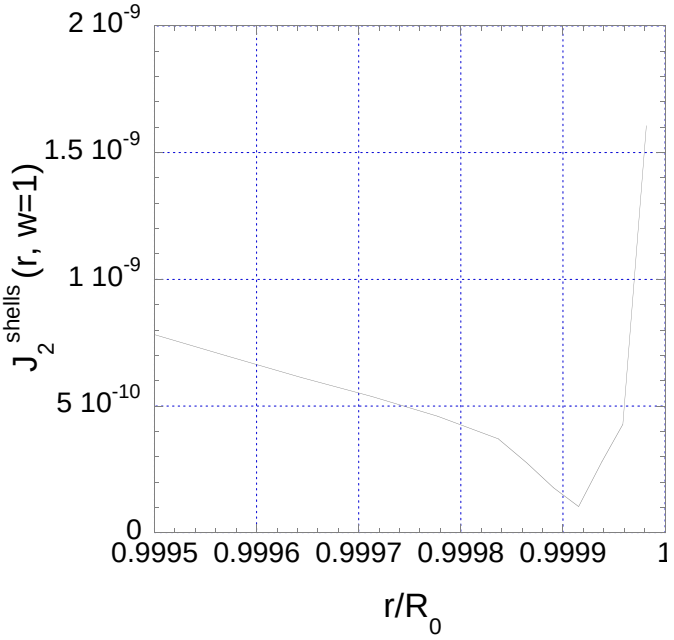

Fig. 1b. Zoom of the right side of the previous profile. Note the minimum which occurs at $0.99992R_\odot$.

in Fig. 1a., which gives the general profile of J_2 from the core to the surface. This profile shows that the quadrupole moment increases almost regularly from $0.3R_\odot$ to $\sim 0.9R_\odot$. Nevertheless, it presents an anomaly at $\sim 0.7R_\odot$ which is certainly due to the transition zone. On one side of the profile, i.e. below $0.3R_\odot$, as previously seen, the knowledge of the core rotation is insufficient to deduce J_2. On the other side, i.e. near the surface, it can be seen that the contribution of the shells is the most significant at $0.9R_\odot$. Beyond this value, the curve decreases down to $0.99992R_\odot$ and increases again up to the surface (Fig. 1b.). In this case, the integrated value of J_2 is given in Fig. 5., according to the computations described in the next section.

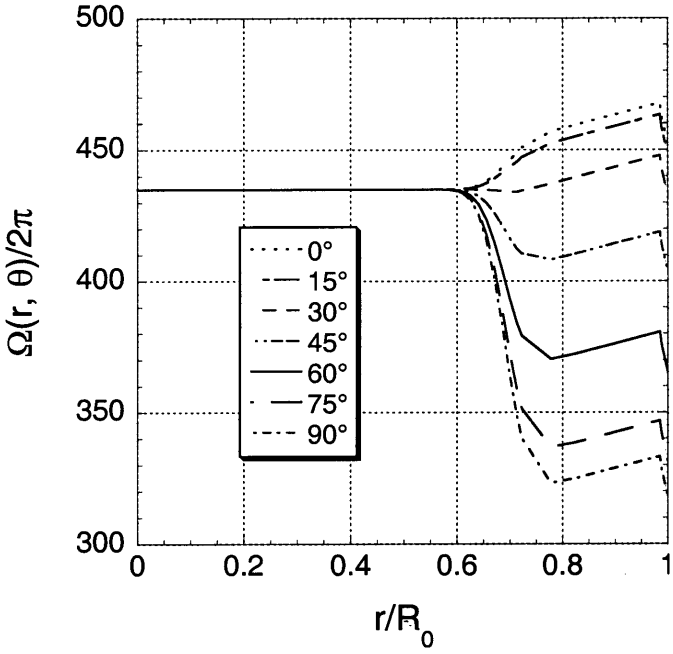

Fig. 2. Solar differential rotation law after Kosovichev (1996) – The rotation rate is expressed in nHz and is drawn for the latitudes 0, 15, 30, 45, 60, 75 and 90 degrees.

3.3. The differential rotation case

The solar differential rotation is now taken into account through Eq. 9 with the dimensionless rotation rate:

$$w(x,\theta) = \frac{\Omega(x,\theta)}{2\pi} \cdot \frac{2\pi}{\Omega_\odot} \tag{20}$$

and is represented in Fig. 2. If the rotation rate is constant from the center up to $0.6R_\odot$, the figure shows that above $0.6R_\odot$, the rotation becomes differential. The region located between 0° and 15° rotates faster than the radiative region (reference speed $\sim$ 435 nHz), and a minimum at 75° and at 90° occurs at around 330 nHz. At 30° and 45°, the rotation rates are close to the reference speed, $\sim$420 and $\sim$440 nHz, respectively. The region located at 60° rotate at an intermediate speed of $\sim$370 nHz. Moreover, we notice that all rotation curves show two sets of extrema at $0.72R_\odot$ and $0.985R_\odot$.

Computed with the above mentioned rotation law, Fig. 3a. and Fig. 3b. describe the behavior of J_2, for the successive solar shells and at each of the previously given latitudes.

This computed quadrupole moment behavior is consistent with the differential rotation law which expresses the fact that the higher the rotation rate of a shell, the higher the value of J_2. The sum of the quadrupole moments on each shell yields the

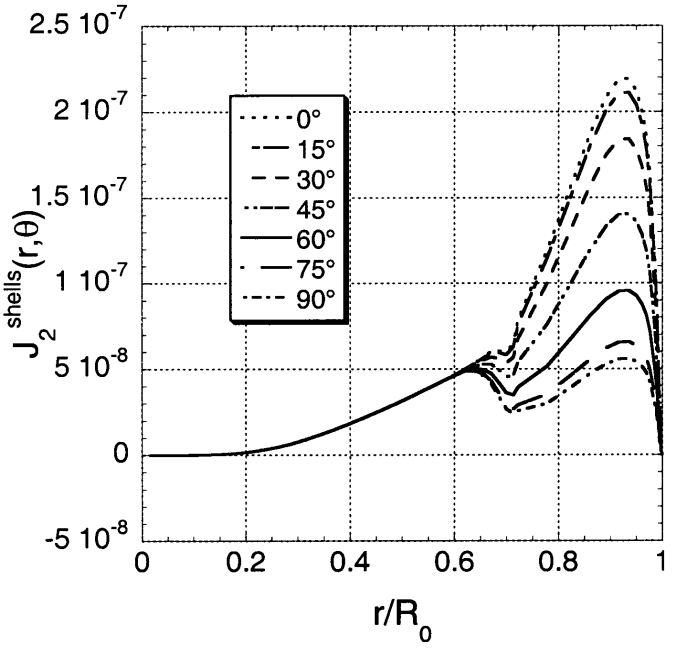

Fig. 3a. Profiles of the quadrupole moment of the Sun splitted in successive shells and numerically computed for the differential rotation case $\Omega(x, \theta)$; curves are given at the latitudes 0, 15, 30, 45, 60, 75 and 90 degrees.

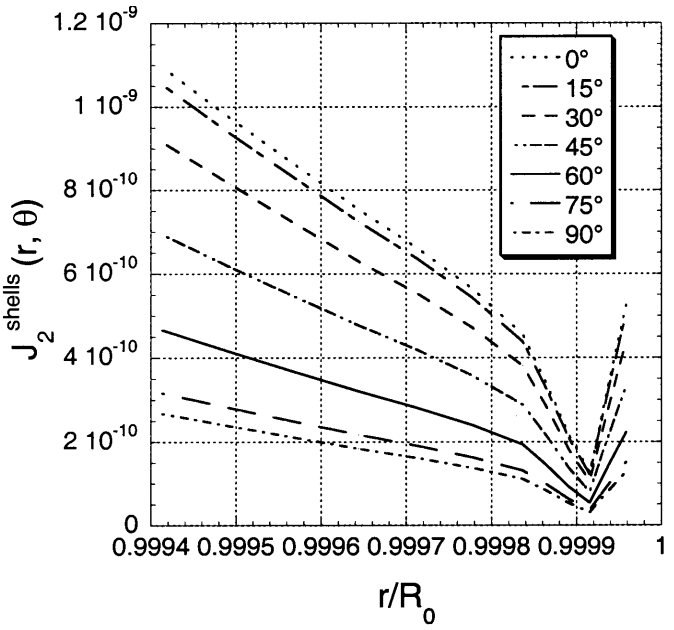

Fig. 3b. Zoom of the right side of the previous profiles. Note the minimum which occurs at the same level 0.99992$R_\odot$ for each heliographic latitude.

behavior of J_2 for a sphere of radius $r_\odot$ that can be expressed at each given latitude (Fig. 4.).

$$J_2(x, \theta') = \sum_{x'} J_2(x', \theta') \triangle x' \tag{21}$$

where x' is associated with the radius of the shells.

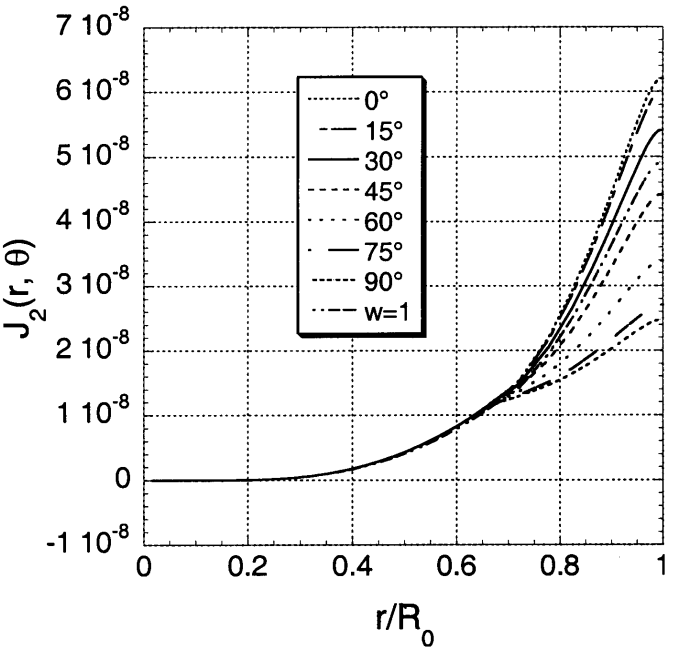

Fig. 4. Profiles of the quadrupole moment of the Sun integrated on successive shells and depending upon the latitudes. By comparison, the case $w = 1$ (rigid rotation) is also given.

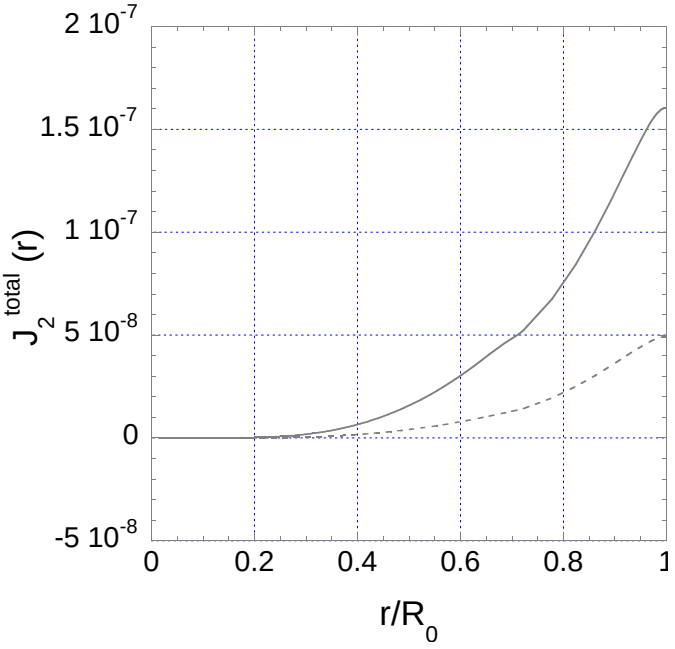

Fig. 5. Profiles of the integrated quadrupole moment of the Sun. The plain curve is computed taken into account the differential rotation. Note the slight but noticeable break in the curve around 0.7$R_\odot$. The dashed curve is obtained in the case of rigid rotation: $w = 1$.

The sum of this quadrupole moment over all the heliographic latitudes yields the total behavior of J_2 (Fig. 5.):

$$J_2(x, \theta) = \sum_{\theta'} J_2(x, \theta') \triangle \theta' \tag{22}$$

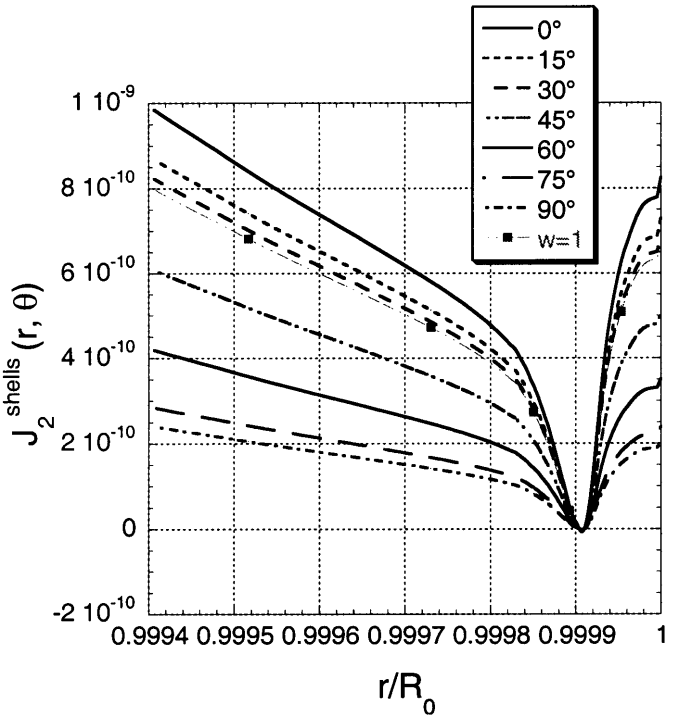

Fig. 6. Profile of the quadrupole moment of the Sun splitted into successive shells and numerically computed for the differential rotation case, using the model of Morel et al. (500 numerical integration steps from r=0.99$R_\odot$ to the surface). The main feature is the minimum which occurs at the level 0.99991$R_\odot$ for each heliographic latitude (0° is the equator).

The model used stops at 0.999985$R_\odot$, but, the curve of the integrated profile shows a plateau that begins around 0.98$R_\odot$, so that J_2 near the surface can be determined as

$$J_2^{surf} \simeq 1.60.10^{-7} \quad (23)$$

The computations of J_2 with a rotation rate of the core equal to 500 nHz and 230 nHz gave respectively $J_2^{surf} \simeq 1.61.10^{-7}$ and $J_2^{surf} \simeq 1.59.10^{-7}$. This result means that the rotation rate of the core does not influence the integrated value of the quadrupole moment of the Sun.

Comparing the profile of J_2 for the differential rotation case with the profile of J_2 in the rigid body case (Fig. 5.), we see that the quadrupole moment is increased by the differential rotation from $0.49.10^{-7}$ to $1.60.10^{-7}$.

3.4. The stability of the solution

The main result obtained by solving Eq. 4 is the non-monotonic behavior of J_2 as displayed in Figs. 1b. and 3b. As a matter of fact, $U(x)$ varies by at least 3 orders of magnitude between $r = 0.99R_\odot$ and $r = 1R_\odot$ and more rapidly near the surface. $V(x)$, which is the result of a derivation process, varies by some 1.5 order of magnitude, so that the product UV may perturb the solution. The sample of 220 shells, used in this paper to scan the whole range of r, could appear insufficient and thus, the decrease obtained around $r = 0.99992R_\odot$ could be a pure numerical effect. To check this point, we made different computations involving the whole process in three ways. We first used the model of density given by Narain et al. (1998) which shows no inflexion point near the surface; $\rho(r)$ can be expressed as a monotonic power law. In that case, as one could expect, no minimum is observed near the surface. In a second step, we used the same model of Richard, but taking into account 800 shells, of which 120 are in the range under consideration, that is to say between $r = 0.99$ and $r = 1R_\odot$. In that case, an extremum in the profile of J_2 has been obtained again, which corresponds to a slight inflexion point in the density profile. Finally, we completely changed the model used in order to compute J_2 with a maximum of shells presently available. Morel et al. (1999) have kindly provided us such a standard solar model sampled by 2100 steps; in this case 500 shells are located between 0.99 and 1$R_\odot$. The result is given in Fig. 6 and shows again a minimum located at 0.99991$R_\odot$. From these above considerations, we conclude that the solution obtained in the previous approach, using the standard Model 3, is self consistent, and retains useful accuracy down to $r = 0.99R_\odot$.

3.5. The quadrupole moment and the internal structure of the Sun

The anomalies, clearly visible in Figs. 3a. and 3b., must be interpreted. The luminosity and the sound speed, which are not directly involved, seem to play an important role. First, the luminosity increases in the core and is constant outside, up to the surface, where it sharply decreases near 0.9998$R_\odot$ and then reaches again its initial constant value. But, can we explain this decrease of the luminosity near the surface by the quadrupole moment? As the luminosity varies also in time, on a time scale of minutes to years, and if the central energy remains constant while the rate of energy emission from the surface varies, there must be an intermediate reservoir, where the energy can be stored or released, depending on the variable rate of energy transport. The gravitational field is one such energy reservoir. If energy is stored in this reservoir, it will impact on the Sun radius, i.e. in the quadrupole moment. Obviously, this needs to be confirmed, but, it may be the first step in understanding a dynamical shape of the Sun (Pap et al., 1998). Second, the sound speed profile given by Richard's model, is consistent with those derived from helioseismic data, whereas they are computed solely with element segregation and no special assumptions added. Indeed, this feature validates his model. What is important, is that near 0.725$R_\odot$ the sound speed sharply decreases. It would be tempting to interpret the steep decrease of J_2 exactly at the same place by the depletion of elements in the Sun (such as beryllium and lithium), which also affects the sound speed. But a model without mixing (Model 3) and a model with mixing (Model 5) yield rigorously the same profile. This suggests that the material redistribution could not be the only physical process which takes place in the transition zone. One possible explanation is the shearing existing between the radiative and the convective zones. Via the Schwarzchild criterion (stipulating that if the actual structural temperature gradient is greater than the adiabatic

gradient in a zone, this zone is convective), the study of the adiabatic and radiative gradients allows us to define the splitting of the Sun into radiative and convective zones. The passage from one zone to another may also explain the anomalies that we observe on the curve of J_2. We can see two such passages, one at $0.725R_\odot$ and the other at $0.99998R_\odot$. Incidently, this spherical splitting into successive regions of real physical meaning validates our theoretical approach.

4. Discussion

In our study, the determination of the integrated value of J_2 over r and θ leads to $J_2 = 1.60.10^{-7}$ at the surface of the Sun. This result is obviously in agreement with the theoretical upper bound of J_2, equal to $3.0.10^{-6}$, obtained by Rozelot & Bois (1998) . As previously seen, this upper bound has been determined from the accurate knowledge of the Moon's physical librations, for which the Lunar Laser Ranging data reach accuracies at the millisecond level. This lunar-spin orbit coupling theory permits one to obtain $J_{2\,\max}$ an order of magnitude better than the one deduced from the precession rate of the perihelion for planets like Mercury (Bursa, 1986), (Pijpers, 1998), (Campbell et al., 1983) or Icarus (Landgraf, 1992). This precession rate, which is affected by the quadrupole moment of the Sun is always used to validate either the observed or the theoretical values of J_2. It must be noted that this effect is not sufficient to determine an accurate upper bound of J_2; based solely on this advance of the perihelion of Mercury, Kislik (1983) found $J_{2\,\max} = 1.08.10^{-5}$, an obviously too large value. The value of $J_{2\,\max} = 3.0.10^{-6}$, still compatible with the observations, permits a noticeable reduction in the range of the J_2 values.

Furthermore, our value of $J_2 = 1.60.10^{-7}$, consistent with the range of values given by Ulrich and Hawkins (see Sect. 1), is slightly weaker but consistent with those deduced from helioseismological observations and given by Pijpers (1998): $J_2 = (2.18\pm0.06).10^{-7}$. The method used may suffer from systematic effects and other observations may lead to a better accuracy. So, it is necessary to perform other experiments directly dedicated to the determination of J_2, such as the Picard mission (Damé et al., 1998) scheduled for mid-2002. In any event, the results should not change the general behavior of J_2 along the solar radius axis.

It must be underlined that the profile of J_2 is direct information through which the total potential of the Sun can be reached. Experiments such as Mercury orbiter mission with a probe orbiting over the planet may help to accurately determine this potential. For the time being, our analysis shows that this potential is perturbed. From Fig. 3a., it can be seen that this perturbation is almost uniform from the center to about $0.6R_\odot$. The potential is then significantly perturbed, especially when the layer rotates rapidly. The layer located between $0.60R_\odot$ and $0.75R_\odot$, where the rotation rate changes from differential rotation in the convection zone to an almost latitudinally independent rotation rate in the radiative interior, is called the tachocline (Spiegel & Zahn, 1992). The helioseismic data show that this region of rapid change, has its center located only slightly below the convective zone (Kosovichev, 1996a) at $(0.692\pm0.005)R_\odot$, and that the thickness of this rather thin layer is $(0.09\pm0.04)R_\odot$. From these values, we note that the tachocline goes roughly from $0.642R_\odot$ to $0.742R_\odot$. In particular, the helioseismic data show that the endpoint of the adiabatically stratified part of the convection zone is located at $(0.713\pm0.003)R_\odot$ (Kosovichev, 1996a), (Christensen-Dalsgaard et al., 1991). Our curves show a minimum at $0.71293R_\odot$. Thus, the first minimum found on the profile of J_2 determines the base of the convection zone. This can also be found on the curve of the integrated value of J_2 (Fig. 5.).

Moreover, our curves (Fig. 3b.) show a second minimum below the surface at $0.99992R_\odot$. This minimum can be associated with the bottom of the convection zone. According to Richard's model, this bottom seems to be located instead near $0.99998R_\odot$. On the basis of these arguments, we suppose that there is another transition layer located just below the surface, the thickness of which has to be determined. This can be tested by an accurate study of the solar ellipticity, since the quadrupole moment is directly linked to the oblateness.

5. Conclusion

In this analysis, we have determined the profile of J_2 from the core to the surface and we have given its theoretical integrated value at the surface. The method used was the computation of the differential equation governing the fluids in hydrostatic equilibrium which accounts for a solar model of mass and density which respect the helioseismic constraints, together with a rotational solar model. This last model has been derived from the helioseismic data. The result of this computation has allowed us to obtain the total potential, which brings together the rotational and gravitational potentials and which is directly linked to the quadrupole moment.

The main results obtained are the following ones:

- The theoretical value of the solar quadrupole moment is $J_2 = 1.60.10^{-7}$.
- From the model used, J_2 can be drawn as a function of the solar radius (assuming the Sun set up of successive homogeneous thin shells), that shows two sharp decreases D_1 and D_2 located, first at $0.725R_\odot$ and second at $0.99992R_\odot$.
- These two decreases are linked to the solar anomalies which appear in the internal structure, due to the shear layers between the radiative and the convective zones, cf. also (Charbonneau et al., 1999). D_1 is associated with the tachocline, which permits the passage from the radiative interior to a convective layer, and D_2 is associated with a layer located just below the surface which permits the passage from this last convective layer to a new radiative one.
- The first decrease $D_1$is located at the same place when using either Richard's Model 3 (element segregation without rotation-induced mixing) or Model 5 (element segregation with rotation-induced mixing). By comparison with the sound speed profile along the radius which shows the same sharp decrease at the same place, it can be assumed that the lithium and beryllium depletion mechanism is not the most credible explanation.

These features seem to be robust, in the sense of not being influenced by the choice of the model used.

The interest of this work lies in the study of the behavior of the solar quadrupole moment versus the radius and the heliographic latitudes. This solar parameter has been very often neglected in the past, because it was rather difficult to determine an accurate value. The improvement of our knowledge of the accuracy of J_2 is certainly due to the fact that, today, we are able to take into account the differential rotation with depth. In fact, the quadrupole moment plays an important role in the accurate computation of several astrophysical quantities, such as the ephemeris of the planets or the perihelion precession of Mercury and other minor planets such as Icarus. Moreover, J_2 is linked to the Parametrized Post-Newtonian parameter and could be a test to find the most exact possible value of the Eddington-Robertson coefficient (γ). Finally, it is necessary to accurately know the value of the quadrupole moment to determinate the shape of the Sun, that is to say its oblateness.

Acknowledgements. The authors are very grateful to L. Paternó for detailed comments on the first version of this paper and especially for his valuable suggestion concerning the investigation of the numerical effects leading to a more extensive discussion in Sect. 3.4.

References

Allen, C. W.: 1976, Astrophysical Quantities, The Athlone press, Third Edition
Brouillet, N.: 1997, Mathématiques Pour la Physique, Dunod (DEUG Sciences), Paris France
Bursa, M.: 1986, Bull. Astron. Inst. **37**, 312
Campbell, L., MacDow, J. C., Moffat, J. W., et al.: 1983, Nature **305**, 508
Charbonneau, P., Christensen-Dalsgaard, J., Henning, R., et al.: 1999, ApJ, To be published
Christensen-Dalsgaard, J., Gough, D. O., and Thompson, M. J.: 1991, ApJ **378**, 413
Damé, L., Hersé, M., Thuillier, G., et al.: 1998, Nagoya Japan, 32nd COSPAR Assembly - Preprint
Dicke, R. H. and Goldenberg, H. M.: 1967, Phys. Rev. Lett. **18(9)**, 313
Dicke, R. H. and Goldenberg, H. M.: 1974, ApJ Suppl. **27**, 131
Goldreich, P. and Schubert, G.: 1968, ApJ **154**, 1005
Hill, H. A., Bos, R. J., and Goode, P. R.: 1982, Physical Review Letters **49(24)**, 1794
Hill, H. A. and Stebbins, R. T.: 1975, ApJ **200**, 471
Kislik, M. D.: 1983, Sov. Astro. Lett. **9(5)**, 296
Kosovichev, A. G.: 1996a, ApJ **469**, 61
Kosovichev, A. G.: 1996b, in J. Provost and F. X. Schmider (eds.), Sounding Solar And Stellar Interiors, pp 97–98, IAU, Kluwer Academic Publishers, Nice France, Symposium No185, Poster Volume
Landgraf, W.: 1992, Solar Physics **142**, 403
Lieske, J. H. and Null, G. W.: 1969, The Astronomical Journal **74(2)**, 297
Lydon, T. J. and Sofia, S.: 1996, Physical Review Letters **76(2)**, 177
Maier, E., Twigg, L., and Sofia, S.: 1992, ApJ **389**, 447
Morel, P., Provost J., et al.: 1999, Private communication
Narain, U., Agarwal, P., and Sharma, R. K.: 1998, Astron. Astrophys. **335**, 719
Pap, J. M., Kuhn, J., Fröhlich, C., et al.: 1998, in A Crossroads for European Solar and Heliospheric Physics, pp 267–271, ESA, Tenerife Canaria, Proceedings, SP-417
Paterno, L., Sofia, S., and Di-Mauro, M. P.: 1996, Astron. Astrophys. **314**, 940
Pijpers, F. P.: 1998, MNRAS **297**, 76
Richard, O., Vauclair, S., Charbonnel, C., et al.: 1996, Astron. Astrophys. **312**, 1000
Rösch, J., Rozelot, J. P., Deslandes, H., et al.: 1996, Solar Physics **165**, 1
Roxburgh, I. W.: 1964, Icarus **3**, 92
Rozelot, J. P. and Bois, E.: 1998, in K. S. Balasubramaniam, J. Harvey, and D. Rabin (eds.), Synoptic Solar Physics, p. 75, ASP Conference Series, New Mexico USA, 18th NSO / Sacramento Peak Summer Workshop, Volume 140
Spiegel, E. A. and Zahn, J. P.: 1992, Astron. Astrophys. **265**, 106
Ulrich, R. K. and Hawkins, G. W.: 1981, ApJ **249**, 831